OPEN

Hemodynamic Patterns Before Inhospital Cardiac Arrest in Critically Ill Children: An Exploratory Study

Ely Erez, BS[1]
Mjaye L. Mazwi, MBChB[2,3]
Alexandra M. Marquez, MD, MSTR[2,3]
Michael-Alice Moga, MD, MSc[2]
Danny Eytan, MD, PhD[1,2,4]

OBJECTIVES: To characterize prearrest hemodynamic trajectories of children suffering inhospital cardiac arrest.

DESIGN: Exploratory retrospective analysis of arterial blood pressure and electrocardiogram waveforms.

SETTING: PICU and cardiac critical care unit in a tertiary-care children's hospital.

PATIENTS: Twenty-seven children with invasive blood pressure monitoring who suffered a total of 31 inhospital cardiac arrest events between June 2017 and June 2019.

INTERVENTIONS: None.

MEASUREMENTS AND MAIN RESULTS: We assessed changes in cardiac output, systemic vascular resistance, stroke volume, and heart rate derived from arterial blood pressure waveforms using three previously described estimation methods. We observed substantial prearrest drops in cardiac output (population median declines of 65–84% depending on estimation method) in all patients in the 10 minutes preceding inhospital cardiac arrest. Most patients' mean arterial blood pressure also decreased, but this was not universal. We identified three hemodynamic patterns preceding inhospital cardiac arrest: subacute pulseless arrest ($n = 18$), acute pulseless arrest ($n = 7$), and bradycardic arrest ($n = 6$). Acute pulseless arrest events decompensated within seconds, whereas bradycardic and subacute pulseless arrest events deteriorated over several minutes. In the subacute and acute pulseless arrest groups, decreases in cardiac output were primarily due to declines in stroke volume, whereas in the bradycardic group, the decreases were primarily due to declines in heart rate.

CONCLUSIONS: Critically ill children exhibit distinct physiologic behaviors prior to inhospital cardiac arrest. All events showed substantial declines in cardiac output shortly before inhospital cardiac arrest. We describe three distinct prearrest patterns with varying rates of decline and varying contributions of heart rate and stroke volume changes to the fall in cardiac output. Our findings suggest that monitoring changes in arterial blood pressure waveform-derived heart rate, pulse pressure, cardiac output, and systemic vascular resistance estimates could improve early detection of inhospital cardiac arrest by up to several minutes. Further study is necessary to verify the patterns witnessed in our cohort as a step toward patient rather than provider-centered definitions of inhospital cardiac arrest.

KEY WORDS: cardiac arrest; cardiac output; monitoring; patient-centered care; stroke volume; systemic vascular resistance

Cardiopulmonary arrest in childhood is a devastating complication (1,2). The vast majority of events occur in the hospital setting, described as inhospital cardiac arrest (IHCA). Over 15,000 children suffer an IHCA in the United States every year, often associated with poor outcomes (3, 4)

DOI: 10.1097/CCE.0000000000000443

Early warning systems and rapid response teams have led to a change in IHCA location to areas that are more likely to be capable of advanced monitoring and therapeutics, such as the ICU (5). In these settings, clinicians have more access to additional domains of hemodynamic data, such as pulse pressure (PP), heart rate (HR), mean arterial pressure (MAP), oxygen saturation, and end-tidal CO_2, to monitor patient status before, during, and after IHCA.

In recent years, studies of hemodynamic patterns in IHCA helped establish the use of invasive monitoring during cardiopulmonary resuscitation (CPR) (6, 7) and post resuscitative care (8, 9). However, hemodynamic patterns during the prearrest phase of IHCA are poorly characterized and understudied. A better understanding of these patterns may allow more proactive monitoring of at-risk patients, potentially aiding in earlier detection and treatment of IHCA.

IHCA events are marked by a precipitous decline in cardiac output (CO), which stems from a combination of decreases in HR and stroke volume (SV), as well as a compensatory increase in systemic vascular resistance (SVR) to maintain MAP. Although difficult to measure directly, both CO and SVR can be estimated from arterial blood pressure (ABP) waveforms (10). In this exploratory study, we analyzed ABP waveforms associated with IHCA events to characterize the behavior of these derived variables in the phase preceding IHCA, with the aim of determining the potential utility of conducting a larger prospective study in the future.
In this descriptive study, our objectives were to: 1) describe changes in ABP, CO, SV, HR, and SVR preceding IHCA in monitored critically ill children in the ICU setting and 2) determine whether distinct physiologic patterns existed that may facilitate earlier detection and allow for patient-level description of IHCA events.

MATERIALS AND METHODS

Setting and Design

We conducted a retrospective, single-center study at a tertiary-care children's hospital between June 2017 and June 2019. Patient and IHCA event characteristics were obtained from an established IHCA database documenting all ICU-based IHCA events, maintained as part of a continuous quality improvement review and kept in accordance with Utstein guidelines (11). Event waveforms were extracted from a physiologic waveform database known as "AtriumDB." Waveform capture for analysis occurs pervasively for all patients at all times in the Critical Care Units at the Hospital for Sick Children, and data are stored for secondary use (12). Waveform signals associated with a patient are archived in a compressed and time-aligned format for subsequent analysis, as described by Goodwin et al (12). The IHCA documentation database is manually synchronized to AtriumDB by the institution's Cardiac Arrest Review Committee.

Patient Population

All IHCA events occurring in children less than 18 years old in either the PICU or the cardiac critical care unit (CCCU) were eligible for this study. The study was approved with waiver of informed consent by the Research Ethics Board at The Hospital for Sick Children, approval number 1000048904.

To be included in this study, IHCA events were required to involve at least 1 minute of chest compressions or defibrillation and invasive ABP monitoring data for 1 hour before CPR onset and during CPR. Events were excluded if more than 10 minutes of data were missing in the hour preceding CPR or more than 1 minute was missing from the final 15 minutes preceding CPR.

Waveform Analysis

All data were deidentified prior to analysis. Analysis was performed using Matrix Laboratory (MATLAB) Version R2018a (The Mathworks, Natwick, MA). Pulse detection was performed using the automated peak and trough–detection software developed for this project, which was able to identify diastolic minimum timepoints and filter out local outlier values and time points that create a signal with nonphysiologic parameters (e.g., HR greater than 300, no systolic peak). This algorithm achieved better results than similar open-source algorithms for pulse detection, for example, by Zong et al (13) modified with pediatric parameters. Beat-to-beat features, including systolic pressure, diastolic pressure, MAP, systolic time, and diastolic time, were extracted using Sun et al's (14) open-source MATLAB code (15). Outlier values were removed, and the features were smoothed using a moving median.

We selected three previously described CO-estimation algorithms to use for CO trajectory estimation. These methods require calibration to

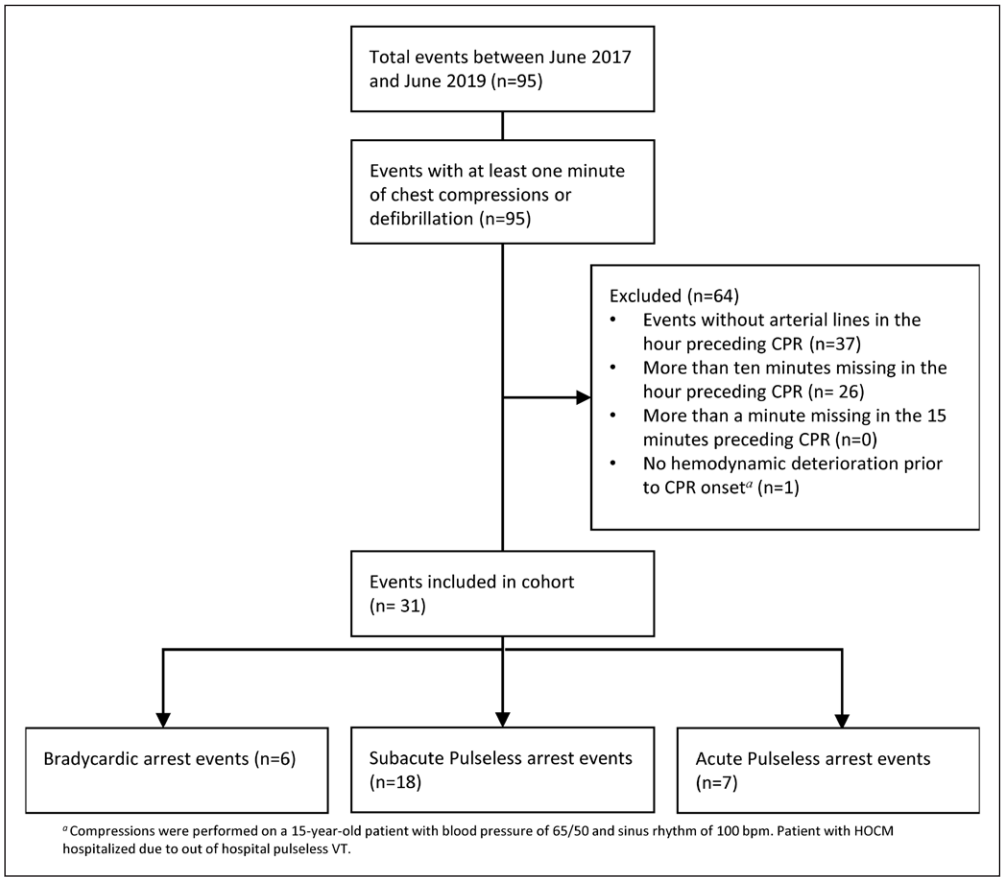

Figure 1. Consolidated Standards of Reporting Trials-style flowchart of inhospital cardiac arrest events divided by prearrest trajectory pattern. CPR = cardiopulmonary resuscitation.

estimate absolute CO accurately, but for the purpose of this study, we were more interested in assessing vectors of changes in CO rather than reporting specific values. Calibration is not indicated with this purpose in mind. Additional information regarding the methods' validation can be found in the **Supplemental Material** (http://links.lww.com/CCX/A660). The first estimate, CO = $k \times$ PP $\times$ HR, was chosen for its simplicity. Proposed by Erlanger and Hooker (16) in 1904, this method is based on the assumption that PP is proportional to SV under constant arterial compliance. The second estimate, proposed by Parlikar et al (17), uses the intrabeat and interbeat variabilities in ABP to estimate the time-constant of a beat-to-beat averaged Windkessel model of the arterial tree, from which an uncalibrated estimate of CO can be obtained.

The third estimate is a modification we developed of a method proposed by Fazeli and Hahn (18). This method assumes that the cardiac ejection phase during systole is rectangular, a more realistic approximation than other Windkessel-based models that assume an instantaneous cardiac ejection phase. Using this assumption, it is possible to derive the equations relating vascular resistance, arterial compliance, systole duration, and the observed systolic and diastolic pressures to an expected ABP waveform contour. SVR is then estimated by finding the values that minimize the absolute differences between the observed (beat-to-beat pulse contour) and expected waveforms using a simplex search method (19). Once SVR is estimated, CO is then proportional to the MAP divided by SVR.

Arterial compliance was assumed to be constant during the hour preceding IHCA. In an unstable child with varying blood pressure (BP), sympathetic tone, and medications, this assumption may be controversial. Little research exists on arterial compliance in unstable children. Evidence suggests that compliance in children and adults is constant under physiologic BP values and may decrease under lower BP values (20–22). Similarly, sympathetic tone has been shown to decrease compliance via arterial smooth muscle contraction (23–25). We believe that compliance either remains constant or decreases preceding arrest, meaning that our estimates likely underestimate CO and SV decreases.

All variables were calculated beat by beat. MAP was calculated by the mean of the waveform values. PP was calculated by the difference between SBP and DBP. SVR estimates were calculated by dividing MAP by CO for Erlanger and Parlikar. SV trajectories are proportional to the PP trajectories under the assumption of constant arterial compliance. HR was calculated by the difference between the consecutive diastole times.

Data and Measurements

We defined the arrest onset time using a patient-based measure called "arterial waveform-derived arrest onset

TABLE 1.
Patient and Event Characteristics by Prearrest Trajectory Group

Patient Characteristics	Overall (*n* = 27)	Subacute pulseless arrest (*n* = 17)	Bradycardic arrest (*n* = 5)[a]	Acute pulseless arrest (*n* = 6)[a]
Age, yr, median (IQR)	0.47 (0.04–0.89)	0.47 (0.02–1.04)	0.98 (0.54–3.36)	0.09 (0.03–0.4)
Age, yr, *n* (%)				
<1	20 (74)	12 (71)	3 (60)	6 (100)
≥1	7 (26)	5 (29)	2 (40)	0
Male, *n* (%)	17 (63)	10 (59)	4 (80)	4 (67)
Illness category, *n* (%)				
Surgical cardiac (postoperative [%])	21 (78)	13 (76) (12 [71])	3 (60) (3 [60])	6 (100) (5 [83])
Medical cardiac	3 (11)	3 (18)	0	0
Surgical noncardiac	0	0	0	0
Medical noncardiac	3 (11)	1 (6)	2 (40)	0
Survival, *n* (%)				
ICU discharge	13 (48)	7 (41)	2 (40)	4 (67)
Hospital discharge	11 (41)	7 (41)	1 (20)	3 (50)
Event Characteristics	Overall (n = 31)	Subacute Pulseless Arrest (*n* = 18)	Bradycardic Arrest (*n* = 6)	Acute Pulseless Arrest (*n* = 7)
Location of CPR event, *n* (%)				
PICU	3 (10)	1 (6)	2 (33)	0
Cardiac critical care unit	28 (90)	17 (94)	4 (67)	7 (100)
Initial AWAO rhythm, *n* (%)				
Pulseless electrical activity	16 (52)	16 (89)	0	0
Asystole	2 (6)	0	0	2 (29)
Narrow complex tachycardia	2 (6)	0	0	2 (29)
Wide complex tachycardia	4 (13)	2 (11)	0	2 (29)
Ventricular fibrillation	1 (3)	0	0	1 (14)
Bradycardia	6 (19)	0	6 (100)	0
Baseline prearrest hemodynamics, median (IQR)				
Mean MAP, mm Hg	47.9 (42.7–57.7)	44.4 (40.1–50.4)	52.9 (49.0–56.3)	53.5 (47.5–60.4)
Mean pulse pressure, mm Hg	34.3 (25.1–44.9)	25.9 (17.5–48.6)	43.0 (41.3–52.7)	32.7 (31.7–39.6)
Mean heart rate, beats/min	128.2 (120.6–151.3)	130.2 (116.4–153.9)	126.6 (122.6–145.5)	144 (126.9–146.4)
AWAO time hemodynamics, median (IQR)				
MAP, mm Hg	32.0 (27.2–36.3)	32.0 (25.6–33.0)	57.4 (39.3–72.0)	26.8 (24.3–33.8)
Pulse pressure, mm Hg	9.8 (9.1–12.5)	9.6 (9.2–11.1)	29.9 (22.6–47.9)	8.8 (7.5–9.9)
Heart rate, beats/min	116 (75.5–140.5)	121.5 (107.6–137.1)	58.5 (55.8–59)	141 (114.5–199.5)

(*Continued*)

TABLE 1. (*Continued*).
Patient and Event Characteristics by Prearrest Trajectory Group

Patient Characteristics	Overall (*n* = 27)	Subacute pulseless arrest (*n* = 17)	Bradycardic arrest (*n* = 5)[a]	Acute pulseless arrest (*n* = 6)[a]
% Declines at AWAO time, median (IQR)				
MAP	38 (23–50)	36 (23–47)	−4 (−53 to 37)	54 (50–61)
Pulse pressure	63 (52–81)	63 (41–77)	28 (−7 to 56)	77 (73–79)
Heart rate	15 (2–45)	12 (4–20)	54 (52–61)	−23 (−49 to 19)
% Declines at CPR onset time, median (IQR)				
MAP	45 (36–53)	49 (36–56)	37 (3–42)	49 (46–57)
Pulse pressure	62 (45–76)	64 (50–78)	38 (23–57)	75 (52–78)
Heart rate	31 (14–58)	34 (17–54)	58 (35–64)	26 (−10 to 28)
% CO declines at AWAO time, median (IQR)				
Modified Fazeli	84 (65–89)	79 (57–86)	90 (81–95)	87 (83–100)
Parlikar	65 (52–81)	62 (53–80)	81 (59–82)	60 (49–71)
Erlanger	67 (52–81)	65 (50–80)	73 (50–81)	70 (58–79)
% CO declines at CPR onset time, median (IQR)				
Modified Fazeli	86 (73–95)	87 (73–96)	86 (80–93)	85 (73–95)
Parlikar	59 (45–74)	58 (46–73)	63 (42–77)	58 (48–71)
Erlanger	80 (68–85)	82 (72–87)	75 (62–82)	74 (68–81)
% Systemic vascular resistance increase at AWAO time, median (IQR)				
Modified Fazeli	240 (108–388)	189 (80–292)	886 (397–1,306)	167 (131–212)
Parlikar	70 (45–172)	81 (50–155)	294 (187–324)	32 (−14 to 53)
Erlanger	126 (57–232)	92 (30–260)	232 (147–260)	146 (61–159)

AWAO = arterial waveform-derived arrest onset, CO = cardiac output, CPR = cardiopulmonary resuscitation, IQR = interquartile range, MAP = mean arterial pressure.
[a]One patient suffered from both a bradycardic arrest and an acute pulseless arrest.

(AWAO)." AWAO employed hemodynamic surrogates for the AHA's clinical criteria for CPR initiation (26) to locate the earliest time each patient qualified for CPR. Patients needed to meet one of the two criteria: the first criterion was severe bradycardia, with an HR below 60, and the second criterion represented pulseless arrest, defined by a PP less than 10 mm Hg and systolic BP less than 50 mm Hg (40 mm Hg for infants less than 1 year old). This criterion for pulseless arrest was used previously by the Collaborative Pediatric Critical Care Research Network in their Pediatric Intensive Care Quality of CPR studies (27–29). We used AWAO rather than the clinician-recorded IHCA onset for several reasons. First, research shows that clinician-reported IHCA times are inaccurate, often due to delays in documentation, inaccurate recollection, and poor synchrony between the clocks used for documentation (30–32). Second, studies have shown that patients often deteriorate prior to the reported IHCA times (33, 34). Third, AWAO is an objective, patient-based definition that can be directly determined form arterial waveforms.

CPR onset time was determined by the characteristic appearance of chest compression or defibrillation

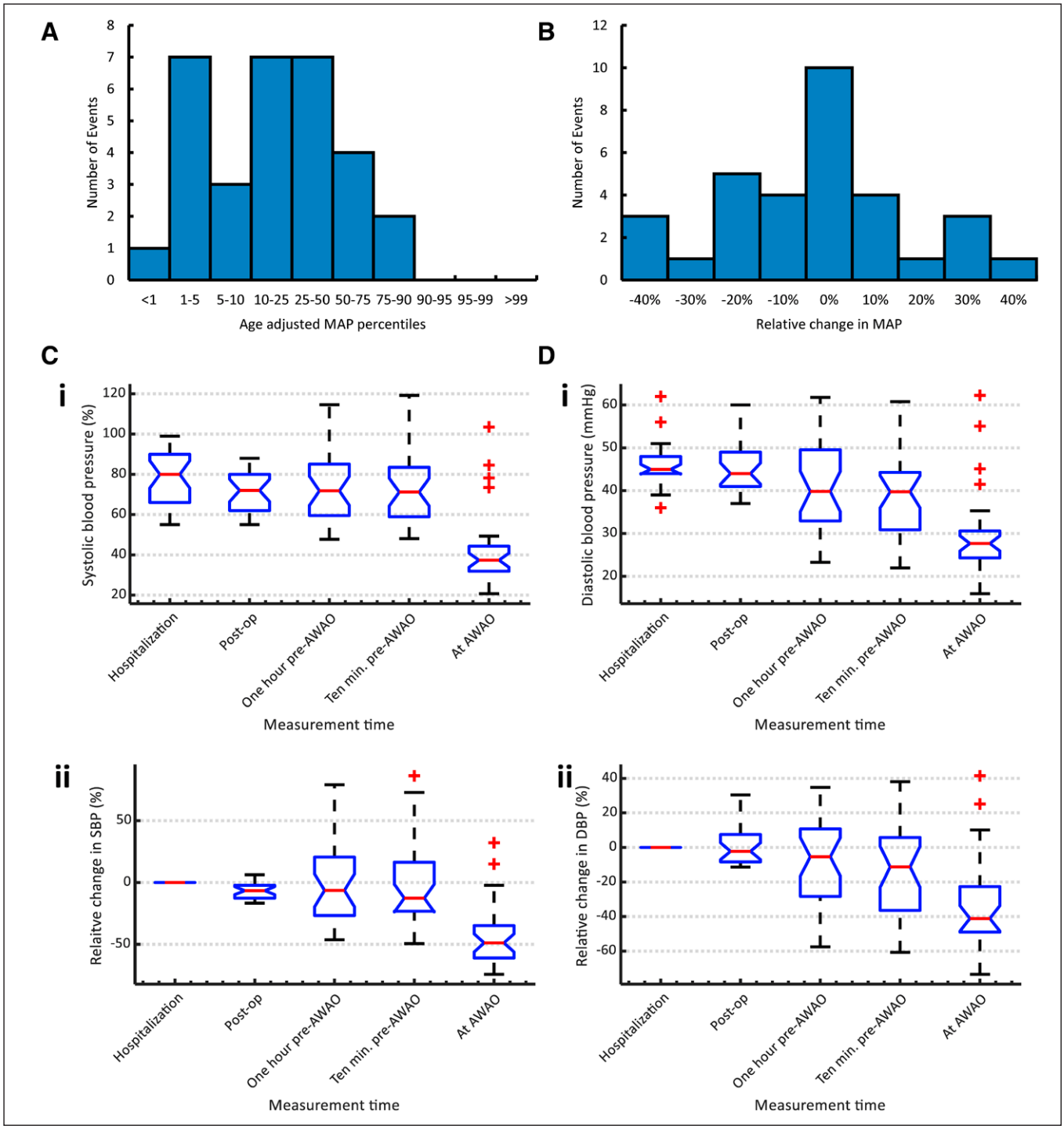

Figure 2. Patient blood pressure characteristics. **A**, Distribution of the age-adjusted mean arterial pressure (MAP) percentiles of the in hospital cardiac arrest events in the cohort. **B**, Distribution of relative percent changes in MAP in the first 50 min of the hour preceding arterial waveform-derived arrest onset (AWAO). **C,** Systolic blood pressure (SBP) (**i**) and percent change in SBP (**ii**) measured at hospitalization, postop (in surgical patients), 1 hour preceding AWAO, 10 minutes preceding AWAO, and at AWAO. **D**, Diastolic blood pressure (DBP) (**i**) and percent change in DBP (**ii**) at the measured times.

on the ABP and electrocardiogram (ECG) waveforms. CPR onset times were used to assess time to CPR initiation and hemodynamic changes occurring late during IHCA. In patients who received CPR before meeting the AWAO criteria, the CPR onset time was used as the AWAO time, and therefore, the time to CPR was zero.

The baseline reference values for each measurement were the mean values from 15 to 10 minutes preceding

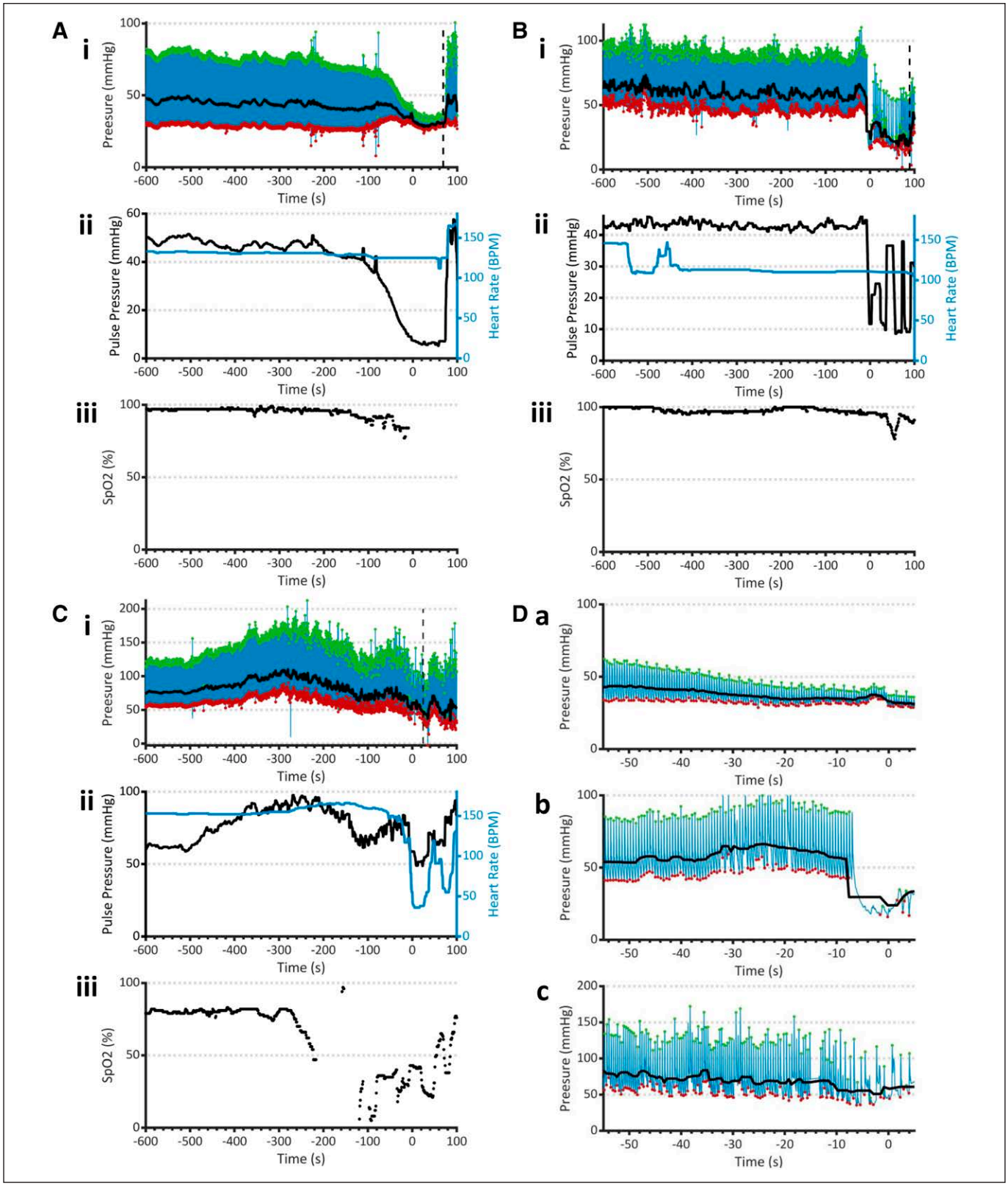

Figure 3. Sample cardiac arrest events. **A–C**, Arterial blood pressure waveform, oxygen saturation, and extracted features in the 10 minutes preceding arterial waveform-derived arrest onset (AWAO; time zero in this figure). Three representative events, one from each group: (**A**) subacute pulseless arrest, (**B**) acute pulseless arrest, and (**C**) bradycardic arrest. In **A–C**: (**i**) Arterial waveform in *blue*, systolic blood pressure in *green*, diastolic blood pressure in *red*, mean arterial pressure in *black*, and *vertical dashed line marks* arterial waveform-derived arrest onset; (**ii**) pulse pressure in *black* and heart rate in *blue*; and (**iii**) oxygen saturation. (**D**) Closeups of (**i**) for the three respective events in the minute preceding AWAO.

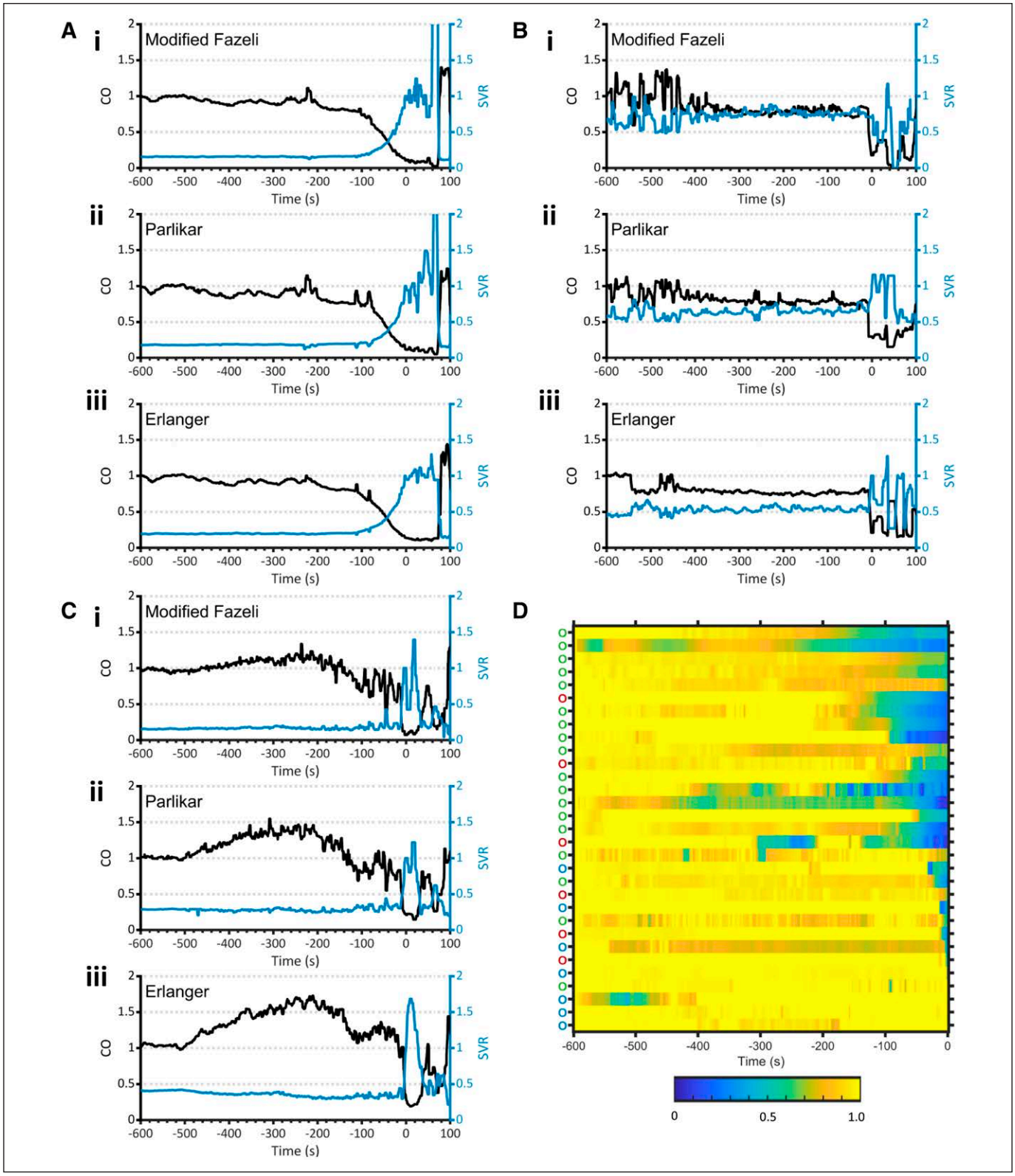

Figure 4. Sample cardiac output (CO) and systemic vascular resistance (SVR) estimates. Sample events shown over the 10 minutes preceding arterial waveform-derived arrest onset. Same events as Figure 3: **A,** subacute pulseless arrest, (**B**) acute pulseless arrest, and (**C**) bradycardic arrest. (**i**–**iii**) CO and SVR for the modified Fazeli, Parlikar, and Erlanger methods, respectively. **D**, Each row represents the Erlanger cardiac output estimate trajectory for an event in the 10 minutes preceding arrest, normalized to baseline cardiac output, sorted by rate of decline and color coded. *Y*-axis label colors in *dots* correspond to prearrest trajectory type: subacute pulseless arrest in *green*, acute pulseless arrest in *blue*, and bradycardic arrest in *red*. Note: events at the *bottom* of the graph declined quickly; therefore, their declines are difficult to observe in this graph.

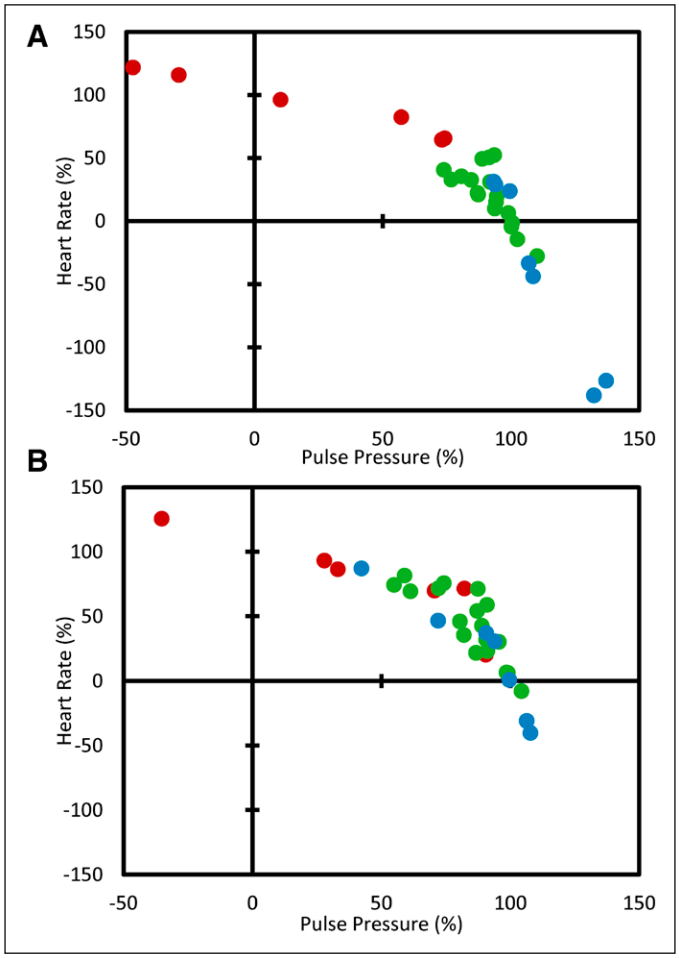

Figure 5. Contributions of changes in pulse pressure or heart rate to decline in cardiac output. Each panel shows the percent change in pulse pressure versus percent reduction in heart rate, each normalized to the percent reduction in cardiac output during the respective timeframes: (**A**) during the 10 min preceding arterial waveform-derived arrest onset time. **B**, During the 10 min preceding cardiopulmonary resuscitation onset time. *Colors* correspond to prearrest trajectory type: subacute pulseless arrest in *green*, acute pulseless arrest in *blue*, and bradycardic arrest in *red*.

AWAO time. This is because assessment of the ABP waveforms revealed that patients' BP values remained relatively stable beforehand and only substantially dropped within the 10 minutes preceding AWAO. We present justification for this decision in the results. Age-adjusted MAP percentiles reported by Eytan et al (35) were used to characterize patient's baseline hemodynamics preceding IHCA.

We identified three prearrest hemodynamic patterns in the ABP waveforms. Events were grouped by the AWAO criterion first met (or most close to meeting at CPR onset) into a bradycardic arrest and a pulseless arrest group. The pulseless group was further divided by rates of decline: events with an immediate disappearance of pulsatile activity were categorized as acute pulseless arrest (within a single beat as observed in the arterial waveform) and the rest as subacute pulseless arrest. Outcomes are reported for the entire cohort and per group.

Statistical Analysis

Primary derived statistics included percent changes in MAP, CO, SVR, PP, and HR from baseline to AWAO time. Secondary ones included the relative contribution of SV and HR to CO decline and time from AWAO time to CPR onset. Due to nonnormal distributions, data are reported as median and interquartile range unless otherwise noted. For the purpose of trajectory estimation, we present CO normalized to each event's baseline CO value and SVR normalized to SVR at AWAO onset time, both in arbitrary units. Wilcoxon signed-rank test was used to compare CO estimates, and Pearson correlation coefficients (r) are reported. Mann-Whitney U test was used to compare changes in the primary derived statistics between the arrest groups. $p < 0.05$ was considered significant.

RESULTS

IHCA Events Characteristics

Out of the 95 events documented in the database, 27 patients with a total of 31 IHCA events (four patients had two events each) were included in this study (**Fig. 1**). **Table 1** shows the characteristics of the subjects and events analyzed. Additional clinical characteristics are presented in **Supplemental Table 1** (http://links.lww.com/CCX/A659). A comparison of patient characteristics of eligible and ineligible IHCA events is presented in **Supplemental Table 2** (http://links.lww.com/CCX/A659). Twenty-eight events (90%) occurred in the CCCU, and three (10%) occurred in the PICU. Twenty-six events (84%) met our AWAO criteria, whereas five events (16%) did not. Events were divided into three groups: 18 subacute pulseless arrests (58%), seven acute pulseless arrests (23%), and six bradycardic arrest (19%). AWAO times were a median of 51 seconds (17.75–82.75 s) earlier than CPR onset times. AWAO-to-CPR onset times were shortest in the bradycardic arrest group (25.5 s [20.9–34.2 s]) followed by the acute pulseless arrest (35 s [13.5–115 s])

and subacute pulseless arrest (55 s [38–120 s]) groups, but these differences were not statistically significant.

Mean Arterial Pressure is Stable, Albeit Relatively Low, in the Hour Preceding IHCA

Patient's baseline MAPs preceding the events were lower than the expected age-specific averages, as shown in **Figure 2**. This figure also shows the relative and absolute change in the values of SBP and DBP for these patients from hospital admission to arrest. The subacute pulseless arrest group had the lowest baseline MAPs an hour prior to cardiac arrest, but this difference did not reach statistical significance (Table 1). During the first 50 minutes of the hour preceding AWAO time, patients' MAPs remained relatively stable with a median decline of only 3.6% (–10 to 15%), with little difference between the groups. In comparison, during the 10 minutes preceding AWAO time, patient's MAPs declined by 38% (23–50%). In that timeframe, 28 events (90%) showed a decline in MAP, whereas 3 (10%) showed an increase in MAP. Events in the acute pulseless arrest group showed the largest decline in MAP with 54% (50–61%) compared with both subacute pulseless arrests (decline of 36% [23–47%], $p < 0.01$) and bradycardic arrests (increase of 4% [–53 to 37%], $p < 0.01$). We focused our analysis on the 10-minute window preceding AWAO time, as all acute decompensation occurred in that timeframe.

Cardiac Arrest is Preceded by a Decline in Cardiac Output

All 31 IHCA events showed marked declines in CO estimates in the 10 minutes preceding AWAO time, with median declines of 84% (65–89%), 65% (52–81%), and 67% (52–81%) in the modified Fazeli, Parlikar, and Erlanger methods, respectively. **Figure 3** shows ABP waveforms and extracted features from three example events, one from each group. The three CO-estimation methods showed strong intermeasure agreement with Pearson *r* values of 0.84, 0.72, and 0.66 between Erlanger and Parlikar, Erlanger and modified Fazeli, and Parlikar and modified Fazeli, respectively. The modified Fazeli method estimated larger declines in CO compared with both the Erlanger ($p < 0.01$) and Parlikar ($p < 0.01$) methods. The decline in CO estimates was very similar among the three IHCA groups, as shown in Table 1. There were no significant differences between the groups in the three estimates, except for the modified Fazeli CO estimates of the acute and subacute IHCA groups ($p = 0.04$). **Figure 4** shows the CO estimates for the three example cases from Figure 3. **Figure 4*D*** presents the normalized Erlanger CO estimates of each of the events sorted by rate of decline. As can be seen in the figure, events in the acute pulseless arrest group showed swift declines in CO over several seconds, whereas events in the bradycardic and subacute pulseless arrest groups showed slower deterioration, with CO declining over several minutes. In the 10 minutes preceding AWAO time, all events in the cohort exhibited a rise in SVR (Table 1). The bradycardic group showed the largest increase in SVR followed by the acute pulseless arrest group and the subacute pulseless arrest group, but these differences did not reach statistical significance.

To better characterize the declines in CO, we assessed the trajectories of its two components, HR and SV (using PP as a proxy) in the prearrest phase. Percent changes in HR and PP for each group are reported in Table 1. **Figure 5** compares the percent change in PP versus the percent change in HR, both normalized to the overall reduction in CO, in the 10 minutes preceding AWAO time and CPR onset time. **Figure 5*A*** shows that, for most patients, the loss of CO is due to a combination of reductions in both HR and PP (i.e., SV) with a wide spectrum of relative contributions. The subacute and acute pulseless arrest groups showed similar behaviors, with decreases in CO mostly attributed to declines in PP. In the bradycardic group, the decreases in CO were mostly attributed to HR. These differences were significant, with bradycardic arrests showing larger declines in HR ($p < 0.01$ compared with both acute and subacute arrests) and smaller declines in PP ($p < 0.01$ and $p = 0.04$ compared with acute and subacute arrests, respectively). **Figure 5*B*** shows that as patients continued to deteriorate, the three groups began to converge; bradycardic events showed a late decrease in PP as subacute and acute pulseless arrest groups showed a decrease in HR.

DISCUSSION

Using arterial waveform analysis of IHCA events in a cohort of critically ill children, we describe a variety of physiologic changes preceding IHCA. Our findings suggest that a substantial decline in CO is a well-conserved

and sensitive herald of impending IHCA and is associated with a compensatory increase in SVR. The decline in CO occurred over seconds to minutes in critically ill patients with relatively unchanged, albeit low, mean BP in the hour prior to cardiac arrest. The percentage decline in CO invariably associated with IHCA was not defined in this study and likely depends on multiple variables including patients' baseline CO and ability to compensate by SVR modulation. Although MAP also decreased preceding IHCA, this decline was not universal, and its magnitude was not consistent. We identified three distinct groups of prearrest hemodynamic patterns. All three groups exhibited similar declines in CO but differed by rates of change and by the relative contributions of HR and SV changes to the decline in CO. Acute pulseless arrests deteriorated over seconds with sharp declines in PP (our surrogate marker for SV) and MAP, mostly due to acute onset arrhythmias. Bradycardic arrests developed more gradually over several minutes and were characterized by HR decreases with preserved PP. These types of arrests are often associated with hypoxia (36). Prearrest oxygen saturation in our bradycardic event cohort are presented in **Supplemental Figure 1** (http://links.lww.com/CCX/A658). Gradual pulseless arrests deteriorated over several minutes with substantial declines in PP. This group was the largest in our cohort, possibly because it was the most common cause of arrest in surgical cardiac patients, which were a larger subset of our cohort compared with similar studies (2, 7, 34, 37, 38). We hypothesize that poor cardiac function with low baseline MAPs and diastolic pressures may make these patients vulnerable to decreases in coronary perfusion pressure leading to IHCA. Attention to maintenance of an adequate coronary perfusion may preserve SV and decrease the risk of IHCA in these vulnerable patients (39). It is important to note that the groups showed convergent behavior as patients continued to deteriorate, eventually lying on a continuum rather than in three distinct clusters (Fig. 5). Therefore, assessing changes in HR or PP separately does not capture the full extent of patients' deterioration.

Measuring exact changes in CO is difficult, even in the ICU setting. Calculating CO using the Fick principal or thermodilution, the current gold standard, requires invasive Swan-Ganz catheterization rarely used in pediatric settings and does not allow for continuous monitoring. Several commercial solutions for estimating CO from ABP waveform exist, but these are not in widespread use nor extensively validated in children (40, 41). Open-source pulse contour-based CO estimates provide a practical alternative for estimating changes in CO, SV, and SVR. Arterial lines, used to record ABP waveforms, are in widespread use in hemodynamically unstable children in the ICU, and there are many available open-source CO estimates (10, 16–18). The three methods we chose rely on different underlying assumptions and require variable computational complexity yet provided consistent estimation of the trajectories of these variables in this population.

Resuscitation has traditionally been focused on clinician-centered improvement efforts such as education, training, and proactive triage of at-risk patients to care environments where more intensive monitoring is possible. Although this approach resulted in significant progress in IHCA prevention and outcomes, improvement has plateaued. We believe a paradigm shift toward patient-centered arrest detection and CPR performance is required to improve outcomes further. Universal guidelines and recommendations are written for the largest possible population of patients and healthcare providers, specifically bystanders responding to an out of hospital cardiac arrest (26, 42). A more nuanced approach can, and should, be applied to intensively monitored patients in specialized environments with highly trained personnel. However, there are no criteria for detecting IHCA based on patients' objective monitored data. Several studies have suggested methods for recognizing deterioration in monitored patients based on combinations of ECG, ABP waveform, pulse oximetry, and end-tidal CO_2, but none have been prospectively validated (28, 33, 34). We believe, based on our findings, that monitoring changes in an expanded range of derived physiologic variables, including proxies for CO, SV, and SVR, may permit more proactive recognition of deterioration and possibly earlier CPR initiation. A better understanding of the underlying physiology leading to arrest in the different subphenotypes may permit targeted treatment for at-risk patients. A larger study is necessary to verify the patterns described in our cohort, as well as to assess the viability of patient-centered IHCA detection in the ICU.

Our study has several key limitations. This is a single-center descriptive study with a small-sized cohort.

No detailed information was reviewed about interventions preceding IHCA. The study cohort included predominantly pediatric cardiac surgical patients, and therefore, our findings may not be generalizable to a pediatric medical patient population. The three CO-estimation methods used in the study have not been validated in children or hemodynamically unstable patients. Hemodynamic instability and variable waveform quality may lead to imperfect pulse detection, potentially skewing CO estimate results. This effect was most prominent in the pulseless phase of the acute pulseless arrest group that exhibited the largest variation between the estimation methods. Overall, we believe the three CO-estimation functions' consistent results suggest that this effect is minor. Our AWAO bradycardia criteria did not account for patients' subjective perfusion assessment by the clinician, potentially selecting early AWAO times in bradycardic patients.

CONCLUSIONS

Our cohort's ABP waveforms exhibited a variety of physiologic changes prior to IHCA. All IHCA events showed a substantial decline in CO occurring shortly before IHCA, with relatively well-preserved BP up until that point. We describe three distinct patterns preceding IHCA with varying rates of decline and varying contributions of HR and SV changes to the declines in CO. Our findings suggest that monitoring changes in ABP waveform-derived HR, PP, CO, and SVR estimates could help detect IHCA earlier by up to several minutes. Further study is necessary to verify and refine the physiologic patterns witnessed in our cohort as a step toward an ultimate goal of patient-centered definitions of IHCA.

1 *Faculty of Medicine, Technion, Haifa, Israel.*

2 *Department of Critical Care Medicine, The Hospital for Sick Children, Toronto, ON.*

3 *Department of Medicine, University of Toronto, Toronto, ON.*

4 *Department of Pediatric Critical Care Medicine, Rambam Medical Center, Haifa, Israel.*

Supplemental digital content is available for this article. Direct URL citations appear in the printed text and are provided in the HTML and PDF versions of this article on the journal's website (http://journals.lww.com/ccejournal).

This research was supported, in part, by the William G. Williams Directorship in Cardiac Analytics and a Canadian Institutes of Health Research/Natural Sciences and Engineering Research Council of Canada (partnered) project grant.

The authors have disclosed that they do not have any potential conflicts of interest.

Address requests for reprints to: Danny Eytan, MD, PhD, Department of Critical Care Medicine, The Hospital for Sick Children, 555 University Ave. 2nd Floor, Atrium - Room 2830A Toronto, ON M5G 1X8, Canada. E-mail: danny.eytan@technion.ac.il;biliary.colic@gmail.com

This research was conducted as part of E. Erez's *Medical Doctor training at the Technion Medical School.*

REFERENCES

1. Martinez PA, Totapally BR: The epidemiology and outcomes of pediatric in-hospital cardiopulmonary arrest in the United States during 1997 to 2012. *Resuscitation* 2016; 105:177–181
2. Berg MD, Nadkarni VM, Zuercher M, et al: In-hospital pediatric cardiac arrest. *Pediatr Clin North Am* 2008; 55:589–604, x
3. Holmberg MJ, Ross CE, Fitzmaurice GM, et al; American Heart Association's Get With The Guidelines–Resuscitation Investigators: Annual incidence of adult and pediatric in-hospital cardiac arrest in the United States. *Circ Cardiovasc Qual Outcomes* 2019; 12:e005580
4. Girotra S, Spertus JA, Li Y, et al; American Heart Association Get With the Guidelines–Resuscitation Investigators: Survival trends in pediatric in-hospital cardiac arrests: An analysis from Get with the guidelines-resuscitation. *Circ Cardiovasc Qual Outcomes* 2013; 6:42–49
5. Nadkarni VM, Larkin GL, Peberdy MA, et al; National Registry of Cardiopulmonary Resuscitation Investigators: First documented rhythm and clinical outcome from in-hospital cardiac arrest among children and adults. *JAMA* 2006; 295:50–57
6. Sheak KR, Wiebe DJ, Leary M, et al: Quantitative relationship between end-tidal carbon dioxide and CPR quality during both in-hospital and out-of-hospital cardiac arrest. *Resuscitation* 2015; 89:149–154
7. Berg RA, Sutton RM, Reeder RW, et al; Eunice Kennedy Shriver National Institute of Child Health and Human Development Collaborative Pediatric Critical Care Research Network (CPCCRN) PICqCPR (Pediatric Intensive Care Quality of Cardio-Pulmonary Resuscitation) Investigators: Association between diastolic blood pressure during pediatric in-hospital cardiopulmonary resuscitation and survival. *Circulation* 2018; 137:1784–1795
8. Moler FW, Holubkov R, Dean JM: Therapeutic hypothermia in children. *N Engl J Med* 2015; 373:980
9. Kilgannon JH, Roberts BW, Jones AE, et al: Arterial blood pressure and neurologic outcome after resuscitation from cardiac arrest*. *Crit Care Med* 2014; 42:2083–2091
10. Sun JX, Reisner AT, Saeed M, et al: The cardiac output from blood pressure algorithms trial. *Crit Care Med* 2009; 37:72–80
11. Zaritsky A, Nadkarni V, Hazinski MF, et al: Recommended guidelines for uniform reporting of pediatric advanced life support: The Pediatric Utstein Style. A statement for healthcare professionals from a task force of the American Academy of

Pediatrics, the American Heart Association, and the European Resuscitation Council. *Resuscitation* 1995; 30:95–115

12. Goodwin AJ, Eytan D, Greer RW, et al: A practical approach to storage and retrieval of high-frequency physiological signals. *Physiol Meas* 2020; 41:035008
13. Zong W, Heldt T, Moody GB, et al: An open-source algorithm to detect onset of arterial blood pressure pulses. *In*: *Computers in Cardiology*, Washington, DC, IEEE Computer Society, 2003
14. Sun JX, Reisner AT, Saeed M, et al: Estimating cardiac output from arterial blood pressure waveforms: A critical evaluation using the MIMIC II database. *In*: *Computers in Cardiology*, Washington, DC, IEEE Computer Society, 2005
15. Goldberger AL, Amaral LA, Glass L, et al: PhysioBank, PhysioToolkit, and PhysioNet: Components of a new research resource for complex physiologic signals. *Circulation* 2000; 101:E215–E220
16. Erlanger J, Hooker DR: An experimental study of blood-pressure and of pulse-pressure in man. *In*: *Johns Hopkins Hospital Report*, Baltimore, MD, Johns Hopkins University, 1904, pp 147–378
17. Parlikar TA, Heldt T, Ranade GV, et al: Model-based estimation of cardiac output and total peripheral resistance. *In*: *Computers in Cardiology*, Washington, DC, IEEE Computer Society, 2007, pp 379–382
18. Fazeli N, Hahn JO: Estimation of cardiac output and peripheral resistance using square-wave-approximated aortic flow signal. *Front Physiol* 2012; 3:298
19. Lagarias JC, Reeds JA, Wright MH, et al: Convergence properties of the Nelder-Mead simplex method in low dimensions. *SIAM J Optim* 1998; 9:112–147
20. Laogun AA, Gosling RG: *In vivo* arterial compliance in man. *Clin Phys Physiol Meas* 1982; 3:201–212
21. Richter HA, Mittermayer C: Volume elasticity, modulus of elasticity and compliance of normal and arteriosclerotic human aorta. *Biorheology* 1984; 21:723–734
22. Langewouters GJ, Wesseling KH, Goedhard WJ: The static elastic properties of 45 human thoracic and 20 abdominal aortas *in vitro* and the parameters of a new model. *J Biomech* 1984; 17:425–435
23. Boutouyrie P, Lacolley P, Girerd X, et al: Sympathetic activation decreases medium-sized arterial compliance in humans. *Am J Physiol* 1994; 267:H1368–H1376
24. Bank AJ, Wilson RF, Kubo SH, et al: Direct effects of smooth muscle relaxation and contraction on *in vivo* human brachial artery elastic properties. *Circ Res* 1995; 77:1008–1016
25. Sonesson B, Vernersson E, Hansen F, et al: Influence of sympathetic stimulation on the mechanical properties of the aorta in humans. *Acta Physiol Scand* 1997; 159:139–145
26. de Caen AR, Berg MD, Chameides L, et al: Part 12: Pediatric advanced life support: 2015 American Heart Association Guidelines Update for Cardiopulmonary Resuscitation and Emergency Cardiovascular Care. *Circulation* 2015; 132:S526–S542
27. Tibballs J, Russell P: Reliability of pulse palpation by healthcare personnel to diagnose paediatric cardiac arrest. *Resuscitation* 2009; 80:61–64
28. Morgan RW, Landis WP, Marquez A, et al: Hemodynamic effects of chest compression interruptions during pediatric in-hospital cardiopulmonary resuscitation. *Resuscitation* 2019; 139:1–8
29. Morgan RW, Reeder RW, Meert KL, et al; Eunice Kennedy Shriver National Institute of Child Health and Human Development/Collaborative Pediatric Critical Care Research Network (CPCCRN) Pediatric Intensive Care Quality of Cardio-Pulmonary Resuscitation (PICqCPR) Investigators: Survival and hemodynamics during pediatric cardiopulmonary resuscitation for bradycardia and poor perfusion versus pulseless cardiac arrest. *Crit Care Med* 2020; 48:881–889
30. McInnes AD, Sutton RM, Nishisaki A, et al: Ability of code leaders to recall CPR quality errors during the resuscitation of older children and adolescents. *Resuscitation* 2012; 83:1462–1466
31. Jones PG, Miles JL: Overcoming barriers to in-hospital cardiac arrest documentation. *Resuscitation* 2008; 76:369–375
32. Park HS, Jung SK, Kim HC: Accuracy of the cardiopulmonary resuscitation registry in an emergency department. *Emerg Med J* 2012; 29:287–289
33. Siems A, Tomaino E, Watson A, et al: Improving quality in measuring time to initiation of CPR during in-hospital resuscitation. *Resuscitation* 2017; 118:15–20
34. Olson M, Helfenbein E, Su L, et al; Revive Initiative at Stanford Children's Health: Variability in the time to initiation of CPR in continuously monitored pediatric ICUs. *Resuscitation* 2018; 127:95–99
35. Eytan D, Goodwin AJ, Greer R, et al: Heart rate and blood pressure centile curves and distributions by age of hospitalized critically ill children. *Front Pediatr* 2017; 5:52
36. Daly MD, Angell-James JE, Elsner R: Role of carotid-body chemoreceptors and their reflex interactions in bradycardia and cardiac arrest. *Lancet* 1979; 1:764–767
37. Meert KL, Donaldson A, Nadkarni V, et al; Pediatric Emergency Care Applied Research Network: Multicenter cohort study of in-hospital pediatric cardiac arrest. *Pediatr Crit Care Med* 2009; 10:544–553
38. Knudson JD, Neish SR, Cabrera AG, et al: Prevalence and outcomes of pediatric in-hospital cardiopulmonary resuscitation in the United States: An analysis of the Kids' Inpatient Database*. *Crit Care Med* 2012; 40:2940–2944
39. Paradis NA, Martin GB, Rivers EP, et al: Coronary perfusion pressure and the return of spontaneous circulation in human cardiopulmonary resuscitation. *JAMA* 1990; 263:1106–1113
40. Esper SA, Pinsky MR: Arterial waveform analysis. *Best Pract Res Clin Anaesthesiol* 2014; 28:363–380
41. Montenij LJ, de Waal EE, Buhre WF: Arterial waveform analysis in anesthesia and critical care. *Curr Opin Anaesthesiol* 2011; 24:651–656
42. Berg MD, Schexnayder SM, Chameides L, et al: Part 13: Pediatric basic life support: 2010 American Heart Association Guidelines for Cardiopulmonary Resuscitation and Emergency Cardiovascular Care. *Circulation* 2010; 122:S862–S875